

# MAS-NMR study of lithium zinc silicate glasses and glass-ceramics with various ZnO content

Madhumita Goswami<sup>a,1</sup>, Govind P. Kothiyal<sup>b</sup>, Lionel Montagne<sup>a,\*</sup>, Laurent Delevoye<sup>a</sup>

<sup>a</sup>UCCS—Unité de Catalyse et Chimie du Solide, UMR CNRS 8181, Ecole Nationale Supérieure de Chimie de Lille, Université des Sciences et Technologies de Lille, BP 108, 59652 Villeneuve d'Ascq Cedex, France

<sup>b</sup>Technical Physics and Prototype Engineering Division, Bhabha Atomic Research Centre, Trombay, Mumbai 400085, India

Received 12 September 2007; received in revised form 16 November 2007; accepted 27 November 2007

Available online 4 January 2008

## Abstract

Lithium zinc silicate glasses of composition (mol%):  $17.5\text{Li}_2\text{O}-(72-x)\text{SiO}_2-x\text{ZnO}-5.1\text{Na}_2\text{O}-1.3\text{P}_2\text{O}_5-4.1\text{B}_2\text{O}_3$ ,  $5.5 \leq x \leq 17.7$ , were prepared by conventional melt-quenched technique and converted to glass-ceramic by controlled crystallization process.  $^{29}\text{Si}$  and  $^{31}\text{P}$  MAS-NMR was used to characterize the structure of both glass and glass-ceramic samples. Despite the complex glass composition,  $Q^2$ ,  $Q^3$  and  $Q^4$  sites are identified from  $^{29}\text{Si}$  MAS-NMR, which relative intensities are found to vary with the ZnO content, indicating a network depolymerization by ZnO. Moreover, well separated  $Q^3$  and  $Q^4$  resonances for low ZnO content indicates the occurrence of phase separation. From  $^{31}\text{P}$  MAS-NMR, it is seen that phosphorus is mainly present in the form of *ortho*-( $Q^0$ ) and *pyro*-phosphate ( $Q^1$ ) structural units and variation of ZnO content did not have much effect on these resonances, which provides an additional evidence for phase separation in the glass. On conversion to glass-ceramics, lithium disilicate ( $\text{Li}_2\text{Si}_2\text{O}_5$ ), lithium zinc *ortho*-silicate ( $\text{Li}_3\text{Zn}_{0.5}\text{SiO}_4$ ), tridymite ( $\text{SiO}_2$ ) and cristobalite ( $\text{SiO}_2$ ) were identified as major silicate crystalline phases. Using  $^{29}\text{Si}$  MAS-NMR, quantification of these silicate crystalline phases is carried out and correlated with the ZnO content in the glass-ceramics samples. In addition,  $^{31}\text{P}$  spectra unambiguously revealed the presence of crystalline  $\text{Li}_3\text{PO}_4$  and  $(\text{Na,Li})_3\text{PO}_4$  in the glass-ceramics.

© 2007 Elsevier Inc. All rights reserved.

**Keywords:** Lithium zinc silicate glass; Glass-ceramics; MAS-NMR; Phase separation

## 1. Introduction

Lithium zinc silicate (LZS) glass-ceramics find wide applications for the fabrication of hermetic glass-ceramic-to-metal (GCM) seals with variety of metals and alloys [1,2] because of their tuneable thermal expansion characteristics ( $50\text{--}200 \times 10^{-7} \text{K}^{-1}$ ). Number of studies has been carried out on the thermo-physical properties of this system [3–14]. For instance, the crystallization behaviour and thermo-physical properties of LZS glass-ceramics with low ZnO content (4.3 mol%) have been reported [8–12]. Schweiger and co-workers [3] have studied the effect of

$\text{P}_2\text{O}_5$  on crystallization and microstructure of this glass-ceramics system. They inferred that the phase transformations and crystallization of lithium disilicate during heating were mainly affected by  $\text{P}_2\text{O}_5$  content of the samples, and that 1.5–2.5 mol%  $\text{P}_2\text{O}_5$  as nucleating agent produces a glass-ceramic with fine grained interlocking microstructures after heat treatment. The influence of  $\text{K}_2\text{O}$  and  $\text{P}_2\text{O}_5$  on crystallization sequence of  $\text{Li}_2\text{O}\text{--}\text{ZnO}\text{--}\text{SiO}_2$  glass-ceramics containing low ZnO content was investigated by McMillan and co-worker [12]. Small addition of  $\text{K}_2\text{O}$  varies the crystallization sequence and the phase composition of resulting glass-ceramics.

Recently, a study on the thermo-mechanical properties of this LZS system with variable ZnO to ZnO +  $\text{SiO}_2$  ratio has been carried out by Sharma et al. [13]. They reported that the thermo-mechanical properties of LZS glass-ceramics are dependent on the bulk composition and subsequently on the major crystalline phases developed

\*Corresponding author.

E-mail address: [lionel.montagne@univ-lille1.fr](mailto:lionel.montagne@univ-lille1.fr) (L. Montagne).

<sup>1</sup>Permanent address: Technical Physics and Prototype Engineering Division, Bhabha Atomic Research Centre, Trombay, Mumbai 400085, India.

during the heat treatment. They have optimized the process parameters to tune the thermal expansion characteristics of LZS glass-ceramics, making them suitable for sealing applications with Cu and stainless steel SS-321 [14]. In a recent work by this group, crystallization behaviour during sealing process for low and high ZnO content samples was also studied with different heat schedules [2].

Since the physico-chemical properties of glass-ceramics are governed by the relative concentration of different crystalline phases as well as on the nature of residual glassy phase, it is important to characterize the local environment of the crystalline and amorphous components formed during conversion of glass to glass-ceramics. Although a number of studies related to various physical and thermo-mechanical properties were carried out on this LZS system, not much work related to the structural aspects of this material using MAS-NMR is available in the literature. Dupree et al. and Holland et al. reported on early stages of crystallization in lithium disilicate glasses containing P<sub>2</sub>O<sub>5</sub> using NMR [15,16]. From the evolution of chemical shifts and relaxation time of Q<sup>4</sup> species, they inferred the presence of liquid–liquid phase separation in lithium silicate glass containing 2wt% P<sub>2</sub>O<sub>5</sub>, which was not detectable even with Transmission Electron Microscopy (TEM).

The aim of our study was to obtain structural data on LZS glass-ceramics developed for sealing applications [13]. Despite the complexity of these multi-component glasses, we managed to characterize phosphorus, silicon and boron speciation in LZS glasses and glass-ceramics with various amounts of ZnO, which will be called “LZSH” hereafter. ZnO was indeed shown to advantageously to replace SiO<sub>2</sub> in the glass composition, leading to thermo-mechanical properties better suited for sealing applications. <sup>29</sup>Si and <sup>31</sup>P MAS-NMR was used to characterize the local environment around the main glass forming elements. Unfortunately, recording <sup>67</sup>Zn solid state-NMR spectra is not possible on these samples since it is a quadrupolar nucleus ( $I = 5/2$ ) with a very low sensitivity ( $1.18 \times 10^{-4}$  vs. <sup>1</sup>H), mainly due to its low Larmor frequency. <sup>7,6</sup>Li, <sup>23</sup>Na and <sup>11</sup>B NMR spectra revealed no useful information in relation with the aim of the present work and will thus not be further mentioned here. We will first report the <sup>29</sup>Si and <sup>31</sup>P NMR spectra of LZSH glasses and of the corresponding glass-ceramics. The different resonances will be assigned to structural units and quantified. The results will then be discussed to highlight two important features for glass-ceramics evaluation: the phase separation in the glasses and the crystallization process.

## 2. Experimental

Lithium zinc silicate glasses of composition (mol%): 17.5Li<sub>2</sub>O–(72– $x$ )SiO<sub>2</sub>– $x$ ZnO–5.1Na<sub>2</sub>O–1.3P<sub>2</sub>O<sub>5</sub>–4.1B<sub>2</sub>O<sub>3</sub>, where  $x$  varied from 5.5 to 17.7 (Table 1), were prepared using 99.7% silica and analytical grade Li<sub>2</sub>CO<sub>3</sub>, KNO<sub>3</sub>, NaNO<sub>3</sub>, H<sub>3</sub>BO<sub>3</sub>, ZnO and (NH<sub>4</sub>)<sub>2</sub>HPO<sub>4</sub> as starting

Table 1  
Nominal compositions of LZSH glasses (mol%)

Sample	SiO <sub>2</sub>	ZnO	Li <sub>2</sub> O	P <sub>2</sub> O <sub>5</sub>	Na <sub>2</sub> O	B <sub>2</sub> O <sub>3</sub>
LZSH1	67.1	5.5	17.0	1.3	5.0	4.1
LZSH2	63.9	8.3	17.3	1.3	5.1	4.1
LZSH3	60.8	11.2	17.4	1.3	5.1	4.2
LZSH4	57.6	14.1	17.6	1.3	5.2	4.2
LZSH5	53.6	17.7	17.8	1.3	5.2	4.3

materials. The batch was subjected to calcination at 850 °C. It was repeated twice after thorough mixing and grinding to ensure the complete mixing and decomposition of the constituents. The charge was then melted in a covered Pt–10% Rh crucible at a temperature of about 1450 °C (depending on the ZnO content) in a raising and lowering hearth furnace and held for 1–2 h for a homogeneous mixing, followed by pouring into a preheated graphite mould. The poured glass was annealed at about 450 °C for 2–4 h before cooling down to room temperature. Clear, transparent and bubble free glasses were obtained for all compositions. These base glasses were converted to glass-ceramics by controlled crystallization using DTA data. The details of the experimental procedure are discussed in our earlier paper [13].

MAS-NMR studies on <sup>29</sup>Si nuclei were carried out using a Bruker Avance 100 spectrometer at a Larmor frequency of 19.8 MHz. The samples were packed in a 7 mm diameter zirconia rotor and subjected to a spinning speed of 4 kHz and a 90° pulse of 2.3 μs duration with a delay time of 180 s. For quantitative measurement, we have recorded spectrum with 20 min delay time and verified that this relaxation delay was sufficient for quantitative measurement. Tetramethylsilane has been used as the reference material for <sup>29</sup>Si MAS-NMR studies. For <sup>31</sup>P MAS-NMR, a Bruker Avance 400 machine was used at a frequency of 161.98 MHz. <sup>31</sup>P NMR spectra were obtained by applying 45° pulse of 2.2 μs duration with a delay of 60 s. The samples were packed in a 4 mm diameter zirconia rotor and spun at the spinning speed of 12.5 kHz. H<sub>3</sub>PO<sub>4</sub> was used as the reference materials for <sup>31</sup>P MAS-NMR. The NMR spectra were decomposed into individual components using the DM-FIT software [17]. Intensities of spinning side bands were included in the deconvolution in order to take into account for the chemical shift anisotropy in the site quantification, and relaxation delays were verified to be long enough to enable sufficient relaxation.

## 3. Results

### 3.1. MAS-NMR of LZSH glasses

<sup>29</sup>Si MAS-NMR spectra for LZSH glass samples with variation of ZnO content are shown in Fig. 1(a). They were decomposed into three individual components centred at  $\delta \approx -80$ ,  $-91$  and  $-110$  ppm (Fig. 1(a)), which are assigned

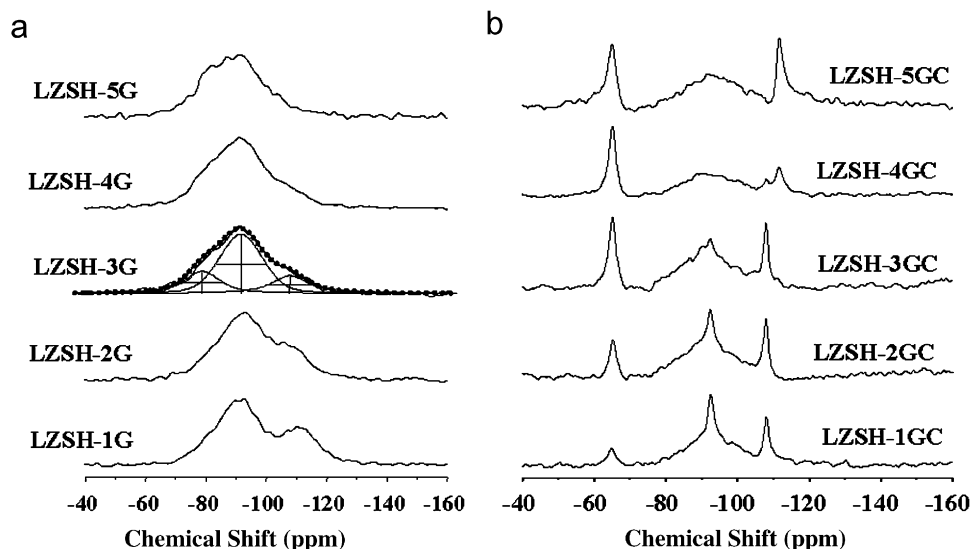


Fig. 1. (a)  $^{29}\text{Si}$  MAS-NMR spectra of LZSH glasses with variation of ZnO content. A typical spectrum deconvolution is shown for LZSH-3G sample. (b)  $^{29}\text{Si}$  MAS-NMR spectra of LZSH glass-ceramics with variation of ZnO content ( $\delta = -64.8$ :  $\text{Li}_3\text{Zn}_{0.5}\text{SiO}_4$ ,  $\delta = -92.25$ :  $\text{Li}_2\text{Si}_2\text{O}_5$ ,  $\delta = -107.73$ : cristobalite,  $\delta = -111.8$ : tridymite).

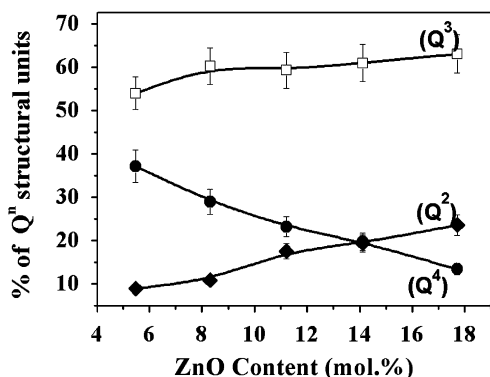


Fig. 2. Variation in relative concentration of silicon  $Q^n$  units with ZnO content. Lines are drawn as a guide to the eye.

to  $Q^2$ ,  $Q^3$  and  $Q^4$  structural units, respectively [18]. The relative amount of these sites vs. ZnO content is plotted in Fig. 2. For increasing amount of ZnO, the amount of  $Q^4$  structural units decreases and that of  $Q^2$  increases, whereas that of  $Q^3$  units remains nearly unchanged (Fig. 2) within deconvolution uncertainty. Fig. 2 thus indicates that for increased amount of ZnO, more non-bridging oxygens are formed at the expense of bridging oxygens of the silicate network. Indeed, increased quantity of  $Q^2$  units (and of  $Q^3$  in less extent) are observed at the expense of  $Q^4$  units (Fig. 2). It is further noticed that there is a shift of  $Q^4$  chemical shift to less negative value as the ZnO content increases. This shift of  $Q^4$  resonance is due to a modification of the second neighbours of  $^{29}\text{Si}$  in these  $Q^4$  sites as more  $Q^2$  and  $Q^3$  sites are formed. The shift of the  $Q^4$  resonance thus confirms the depolymerization of the silica network [19], which is the consequence of the substitution of  $\text{SiO}_2$  for ZnO in the glass formulation

because Si–O–Si groups are replaced by Si–O–Zn (we notice that this schematic view does not involve that Zn has the same structural role that Si).

Fig. 3(a) shows the  $^{31}\text{P}$  MAS-NMR spectra for LZSH glass samples with varying amount of ZnO. All spectra show two broad resonances positioned at 9.5 and  $-1.5$  ppm, with strong and low intensity, respectively. They are assigned to  $Q^0$  and  $Q^1$  structural units, respectively [20]. Whatever the ZnO content of the LZSH glasses, the relative amount of  $Q^0$  sites remains larger than that of  $Q^1$  sites and no significant variation of the intensities is observed. Moreover, only a small shift to larger values is observed for the resonance position of  $Q^0$  and  $Q^1$  with the variation of ZnO content, which suggests that the short range order around  $^{31}\text{P}$  nuclei in the glass samples is not affected by the variation of ZnO content. This point will be further commented in Section 4.

### 3.2. NMR of LZSH glass-ceramics

The  $^{29}\text{Si}$  MAS-NMR spectra of LZSH glass-ceramics samples with variation of ZnO content are shown in Fig. 1(b). Sharp peaks superimposed on a broad resonance are observed on these spectra. The broad resonance between  $-108$  and  $-92.5$  is characteristics of the residual glassy phase present in the glass-ceramic samples, whereas the sharp peaks observed at  $-64.8$ ,  $-92.8$ ,  $-107.7$ , and  $-111.8$  ppm indicate the presence of crystalline phases, in conformity with XRD data [13]. The peak at  $-64.8$  ppm is assigned to the  $Q^0$  silicate sites of lithium zinc *ortho*-silicate ( $\text{Li}_3\text{Zn}_{0.5}\text{SiO}_4$ ) [21], the peak at  $-92.8$  ppm to lithium disilicate ( $\text{Li}_2\text{Si}_2\text{O}_5$ ) [21], the peak at  $-107.7$  ppm to cristobalite ( $\text{SiO}_2$ ) [21], and the peak at  $-111.8$  ppm to tridymite ( $\text{SiO}_2$ ) [21]. The relative intensities of the

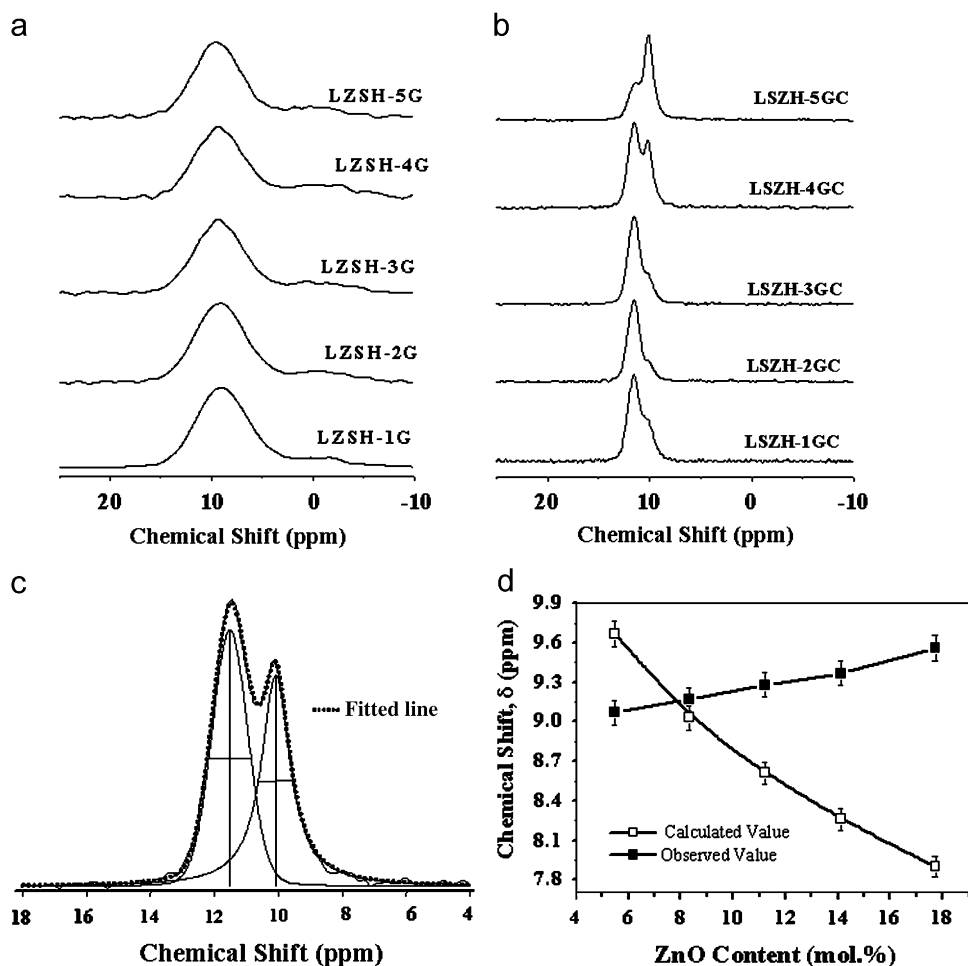


Fig. 3.  $^{31}\text{P}$  MAS-NMR of LZSH (a) glass and (b) glass-ceramic samples with variation of ZnO content. (c) Example of fit of  $^{31}\text{P}$  NMR spectrum of the LZSH4-GC glass-ceramics. The same fit with two different line shapes (Gaussian and Lorentzian) was applied to all spectra. (d) Calculated and observed  $^{31}\text{P}$  NMR chemical shift of  $Q^0$  ortho-phosphate resonances of LZSH glasses with variation of ZnO content.

resonances of the crystalline phases were found to vary with the ZnO content as shown in Fig. 4(a). At low ZnO concentration,  $\text{Li}_2\text{Si}_2\text{O}_5$  is found to be present as the major crystalline phase along with cristobalite and smaller amount of  $\text{Li}_3\text{Zn}_{0.5}\text{SiO}_4$ . When ZnO content increases, the intensity of the peak related to  $\text{Li}_3\text{Zn}_{0.5}\text{SiO}_4$  increases and tridymite is progressively observed in place of cristobalite. The intensity of  $\text{Li}_2\text{Si}_2\text{O}_5$  resonance decreases with ZnO content and finally disappear for higher content of ZnO (17.7 mol%). These variations are in accordance with those previously observed on XRD patterns [13], but NMR enables an easy quantification of the relative amount of different crystalline phases in glass-ceramics samples, as well as the relative amount of residual glassy phase, which are reported in Fig. 4(b).

In Fig. 3(b), two narrow resonances are observed on the  $^{31}\text{P}$  NMR spectra of the glass-ceramics, located at 10.1 and 11.3 ppm, and their relative intensities change with the ZnO content. Since these chemical shifts are out of the range of pyro-phosphate  $Q^1$  units [22], they are assigned to ortho-phosphate  $Q^0$  units. The resonance at 10.1 ppm

is unambiguously assigned to  $\text{Li}_3\text{PO}_4$  [16] crystalline phase. The peak at  $\delta \approx 11.3$  ppm may be assigned to a  $\text{Na}_{3-x}\text{Li}_x\text{PO}_4$  solid-solution because this chemical shift is intermediate between that of  $\text{Na}_3\text{PO}_4$  (13.4 ppm) and  $\text{Li}_3\text{PO}_4$  (10.1 ppm). This situation was already observed in other phosphate solid-solutions [23]. Indeed, the much smaller width of these resonances (half width at half height is 1.1 ppm) compared to that observed in glasses (Fig. 3(a)) suggests that they both stem from crystalline phases and not from residual glassy phase. However, on deconvolution the resonance at 10.1 ppm could be fitted with Lorentzian line shape, but the other one at 11.3 ppm could only be fitted with Gaussian line shape. The former resonance can thus be assigned to the crystalline  $\text{Li}_3\text{PO}_4$  phase, but the Gaussian line shape of the resonance at 11.3 ppm indicates some disorder around the phosphorus site. This disorder probably originates from the variation of  $x$  values because  $\text{Na}_{3-x}\text{Li}_x\text{PO}_4$  is a continuous solid-solution [24]. The evolution of the intensities of the two  $^{31}\text{P}$  resonances (Fig. 3b) indicates that the relative quantity of  $\text{Li}_3\text{PO}_4$  crystals decreases with increased ZnO content in

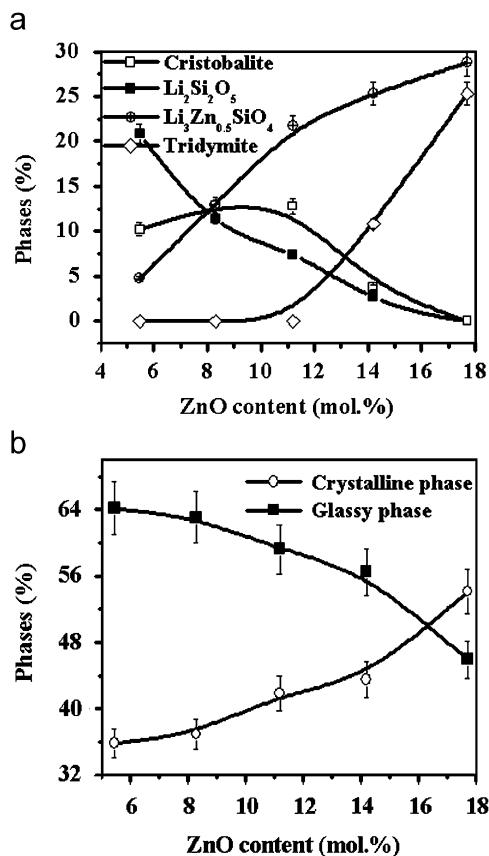


Fig. 4. (a) Percentage of silicate crystalline phases in LZSH glass-ceramics with variation of ZnO content, measured from the relative intensities of  $^{29}\text{Si}$  MAS-NMR spectra. Lines are drawn as a guide to the eye. (b) Percentage of glassy and total silicate crystalline phases in LZSH glass-ceramics with variation of ZnO content, measured from the relative intensities of  $^{29}\text{Si}$  MAS-NMR spectra. Lines are drawn as a guide to the eye.

the glass-ceramics (excepted for the lowest ZnO content). This is probably due to the precipitation of lithium-containing crystalline silicate phases (as discussed in the next section), which decreases the concentration of  $\text{Li}^+$  and thus increases the formation of  $\text{Na}_{3-x}\text{Li}_x\text{PO}_4$ . We noticed that no pure  $\text{Na}_3\text{PO}_4$  phase could be detected in these samples, probably because the  $\text{Na}^+$  concentration is much less than  $\text{Li}^+$  one. We thus conclude that all  $\text{P}_2\text{O}_5$  is involved in crystalline phases in LZSH glass-ceramics and that no  $\text{P}_2\text{O}_5$  could be detected in the remaining glassy phase.

#### 4. Discussion

We have shown in a previous paper that the substitution of ZnO for  $\text{SiO}_2$  in LZSH glasses has large effects on the crystalline phase distribution and on the properties of the glass-ceramics [13]. Thus, the aim of this work was to investigate the structure of these materials before and after crystallization process. Glass-ceramics are obtained by nucleation and crystal growth process. For lithium silicate materials of composition similar to our glasses, nucleation

is often initiated by liquid immiscibility [25]. We will thus separate the discussion of NMR results in two parts: we will first show that solid-state NMR brings information about the occurrence of an amorphous phase separation in these glasses. Then, we will show that in the glass-ceramics both the residual glass phase and the crystalline phases can be characterized with solid-state NMR.

##### 4.1. NMR evidence for amorphous phase separation

The well separated  $Q^3$  and  $Q^4$  resonances on the  $^{29}\text{Si}$  NMR spectra for low ZnO content (Fig. 1(a)) indicate the possibility of some amorphous phase separation. The structural features of a technologically useful multi-components material are complex, since various constituent oxides are added for tuning the characteristics. As a result, the MAS-NMR spectra of such multi-component system are broad and featureless, owing to the large distribution of the environments [26]. Broad and featureless  $^{29}\text{Si}$  resonances could thus be expected for our glasses. Hence, for the higher silica content LZSH glass, the well-resolved  $Q^4$  resonance can be considered as an evidence of silica phase separation during quenching. Phase separation is indeed common in silicate glasses with high silica content [27]. This amorphous phase separation was not detected during the glass formation process (no opacity was visible), and not by microscopic observation with SEM. This phase separation is thus probably limited to the submicron/nanometer range, below the resolution limit of SEM.

A second evidence for amorphous phase separation is provided indirectly by  $^{31}\text{P}$  MAS-NMR.  $^{31}\text{P}$  chemical shift is sensitive to the average field strength of the cation to which phosphorous is coordinated in glass [28]. Since  $\text{Zn}^{2+}$  has a larger field strength than the other modifying cation ( $\text{Na}^+$ ,  $\text{Li}^+$ ), a shift to higher field (more negative chemical shift values) was expected if the *ortho*- or *pyro*-phosphate anions were charge compensated by all the cations present in the glasses. Since the intensities of the  $Q^1$  *pyro*-phosphate resonances remain low whatever the ZnO content is, we could not observe any significant shift for these  $Q^1$  sites on the  $^{31}\text{P}$  NMR spectra (Fig. 3(a)). Nevertheless, significant features could be obtained from  $Q^0$  sites: Fig. 3(d) shows the chemical shift values calculated considering an average distribution of all modifying cations around  $Q^0$  phosphate units. While increasing ZnO content in the glasses, a shift to higher field (i.e. smaller c.s. values) is calculated (assuming a random distribution of cations around phosphate units, c.s. is calculated from  $\delta = \sum c_i \delta_i$ , where  $\delta_i$  is the chemical shift of an *ortho*-phosphate crystalline phase and  $c_i$  is its content in mol%). However, in Fig. 3(d) a shift to lower field is actually observed for measured  $Q^0$  chemical shifts on  $^{31}\text{P}$  NMR spectra. The shift of NMR resonances of the  $Q^0$  *ortho*-phosphates to the opposite side compared to the calculated values (Fig. 3(d)) means that  $\text{Zn}^{2+}$  ions are not bonded to these phosphate anions. Since this is very unlikely in a homogeneous glass and considering previous



studies indicating strong complexation of phosphate anion with divalent cations [29], this is another evidence for the occurrence of a phase separation in glass. Furthermore, this absence of bonding between phosphate and  $\text{Zn}^{2+}$  indicates that ZnO is located in a different phase than that containing the phosphate anions. Since it is known that phosphate anions are located after amorphous phase separation in the less polymerized phase [30], our NMR results suggest that the amorphous phase separation produces a phase rich in  $Q^2$  and  $Q^3$  silicate sites, in which are located phosphate anions and a phase rich in  $Q^4$  and  $Q^3$  silicate sites, which contains most of  $\text{Zn}^{2+}$ . The degree of amorphous phase separation decreases with increasing amount of ZnO in the LZSH glass formulation (as evidenced by less separated  $Q^4$  sites in Fig. 1(a)), probably because the depolymerization of the silica network by ZnO results in less quantity of  $Q^4$  sites.

#### 4.2. NMR analysis of LZSH glass-ceramics

The relative proportion of the different crystalline phases present in LZSH glass-ceramics is dependent on the ZnO content, as was shown qualitatively by XRD [13]. NMR brings complementary information to those XRD results. The quantification of the different crystalline phases is indeed important for optimizing the properties of the glasses, which influences the thermo-mechanical properties of the glass-ceramics [13].

The conversion of LZSH glasses into glass-ceramics results in the presence of sharp resonances  $^{29}\text{Si}$  spectra (Fig. 1(b)), due to crystalline phases. A broad resonance remains on  $^{29}\text{Si}$  spectra of LZSH glass-ceramics, which indicates the presence of residual glassy phase. These  $^{29}\text{Si}$  spectra can be decomposed into individual components, which brings an easy way of quantification of the relative amount of the crystalline and amorphous phases, as shown in Fig. 4(a) and (b). It is observed that the increase of ZnO content in the glasses results in the formation of  $\text{Li}_3\text{Zn}_{0.5}\text{SiO}_4$  crystals at the expense of  $\text{Li}_2\text{Si}_2\text{O}_5$ .  $\text{SiO}_2$  crystalline phases are always present whatever the ZnO content, but cristobalite crystals are observed at low ZnO content and progressive growth of tridymite crystals occurs at higher ZnO content (above 11.2 mol% ZnO). This was already observed in other glass-ceramics [16], but no clear explanation can be given. This could be related to the occurrence of the phase separation in the glass, which induces the formation of a silica-rich phase (as evidenced by  $Q^4$  sites in  $^{29}\text{Si}$  spectra). For larger ZnO content the extent of phase separation is expected to decrease (which is confirmed by less separation of  $Q^4$  sites), and  $\text{SiO}_2$  crystals may be formed through a rearrangement of the silicate network upon crystallization. The glass with highest silica content produces mainly cristobalite and lithium disilicate crystals, which was observed in similar LZS glass-ceramics compositions [31].

$^{31}\text{P}$  NMR shows that the presence of  $\text{Li}_3\text{PO}_4$  and  $\text{Na}_{3-x}\text{Li}_x\text{PO}_4$  crystalline phases has no direct relation with

the ZnO content and with the presence of the different silicate crystalline phases. This is in accordance with previous study [16], which reported that crystalline phosphate is not acting as nucleating agent for crystallization of lithium silicate phases, but it may be indirectly involved by enhancing initial amorphous phase separation in the glass. Our NMR results confirm that such behaviour is also observed in complex glass compositions. NMR was able to detect and quantify a small amount of  $\text{Li}_3\text{PO}_4$  and  $\text{Na}_{3-x}\text{Li}_x\text{PO}_4$  crystals, which could not be detected by XRD. Moreover, NMR is also able to characterize the partition of phosphate between crystal and glassy phase and we have shown that no  $\text{P}_2\text{O}_5$  could be detected in the residual glassy phase in LZSH glass-ceramics.

#### 5. Conclusions

Structural studies using  $^{29}\text{Si}$  and  $^{31}\text{P}$  MAS-NMR were carried out on LZS glass and glass-ceramic samples of nominal glass composition (mol%):  $17.5\text{Li}_2\text{O}-(72-x)\text{-SiO}_2-x\text{ZnO}-5.1\text{Na}_2\text{O}-1.3\text{P}_2\text{O}_5-4.1\text{B}_2\text{O}_3$ , where  $x$  varied from 5.5 to 17.7. We report data on the glass to glass-ceramic conversion involving phase separation and quantification of crystalline phases, which have never been reported on such complex multi-component glass composition.

From  $^{29}\text{Si}$  MAS-NMR spectra, it is observed that  $Q^2$ ,  $Q^3$  and  $Q^4$  structural units are present as a major network forming units in the glass samples and their relative intensities are largely dependent on the amount of ZnO content. For low ZnO content, well separated  $Q^3$  and  $Q^4$  resonances indicate phase separation, which could not be observed from SEM studies. From  $^{31}\text{P}$  MAS-NMR, unchanged resonance positions of the  $Q^0$  and  $Q^1$  phosphorus sites with variation of ZnO content also provides an additional evidence of phase separation in the glass.

Four sharp peaks positioned at  $\delta \approx -64.8$ ,  $-92.8$ ,  $-107.7$  and  $-111.8$  ppm are observed in glass-ceramic samples from  $^{29}\text{Si}$  MAS-NMR spectrum and are identified as  $\text{Li}_3\text{Zn}_{0.5}\text{SiO}_4$ ,  $\text{Li}_2\text{Si}_2\text{O}_5$ , cristobalite and tridymite, in conformity with XRD data. Quantification of silicate crystalline phases using  $^{29}\text{Si}$  MAS-NMR could be possible and it well agrees with the XRD measurements.

Significant information was obtained from  $^{31}\text{P}$  MAS-NMR, which showed that phosphorus is present in two different environments in  $\text{Li}_3\text{PO}_4$  and  $\text{Na}_{3-x}\text{Li}_x\text{PO}_4$  crystals. Since the relative intensity of these resonances does not have any direct relation with the ZnO content and with the growth of different crystalline silicate phases, it can be inferred that  $\text{P}_2\text{O}_5$  is not acting as a nucleating agent for the growth process.

#### Acknowledgments

M. Goswami thanks the USTL for her post-doc grant. The authors also greatly acknowledge B. Revel for his help to carry out NMR measurements. The FEDER, Region

Nord Pas-de-Calais, Ministère de l'Education Nationale de l'Enseignement Superieur et de la Recherche, CNRS, and USTL are acknowledged for funding of NMR spectrometers.

## References

- [1] P.W. McMillan, S.V. Phillips, G. Partridge, *J. Mater. Sci.* 1 (1966) 269.
- [2] M. Goswami, P. Sengupta, K. Sharma, R. Kumar, V.K. Shrikhande, J.M.F. Ferreira, G.P. Kothiyal, *Ceram. Int.* 33 (2007) 863.
- [3] S.C.V. Clausbruch, M. Schweiger, W. Höland, V. Rheinberger, *J. Non-Cryst. Solids* 263/264 (2000) 3884.
- [4] A.A. Omar, A.W.A. El-Shennavi, A.R. El-Ghannam, *J. Mater. Sci.* 26 (1991) 6049.
- [5] C. Wang, W. Xu, *J. Non-Cryst. Solids* 80 (1986) 237.
- [6] E. Demirkesen, E. Maytalan, *Ceram. Int.* 27 (2001) 99.
- [7] Z.X. Chen, P.W. McMillan, *J. Am. Ceram. Soc.* 68 (4) (1985) 220.
- [8] I.W. Donald, B.L. Metcalfe, D.J. Wood, J.R. Copley, *J. Mater. Sci.* 24 (1989) 3892.
- [9] I.W. Donald, B.L. Metcalfe, A.E.P. Morris, *J. Mater. Sci.* 27 (1992) 2979.
- [10] I.W. Donald, *J. Mater. Sci.* 28 (1993) 2841.
- [11] R. Morrell, K.H.G. Ashbee, *J. Mater. Sci.* 8 (1973) 1271.
- [12] Z.X. Chen, P.W. McMillan, *J. Am. Ceram. Soc.* 68 (4) (1985) 220.
- [13] B.I. Sharma, M. Goswami, P. Sengupta, V.K. Shrikhande, G.B. Kale, G.P. Kothiyal, *Mater. Lett.* 58 (2004) 2423.
- [14] G.P. Kothiyal, B. Indrajit Sharma, V.K. Shrikhande, M. Goswami, J.V. Yakhmi, *Key Eng. Mater.* 280–283 (2005) 947.
- [15] R. Dupree, D. Holland, M.G. Mortuza, *J. Non-Cryst. Solids* 116 (1990) 148.
- [16] D. Holland, Y. Iqbal, P. James, B. Lee, *J. Non-Cryst. Solids* 232–234 (1998) 140.
- [17] D. Massiot, F. Fayon, M. Capron, I. King, S. Le Calve, B. Alonso, J.O. Durand, B. Bujoli, Z. Gan, G. Hoatson, *Magn. Reson. Chem.* 40 (2002) 70.
- [18] K.J.D. Mackenzie, M.E. Smith, *Multinuclear Solid-state NMR of Inorganic Materials*, Pergamon Materials Series, vol. 6, Pergamon, Amsterdam, 2002.
- [19] M. Schmucker, K.J.D. Mackenzie, H. Schneider, R. Meinhold, *J. Non-Cryst. Solids* 217 (1997) 99.
- [20] F. Munoz, L. Montagne, L. Delevoye, A. Duran, L. Pascual, S. Cristol, J.F. Paul, *J. Non-Cryst. Solids* 352 (2006) 2958.
- [21] F. Jonathan Stebbins, *Mineral Physics and Crystallography, Handbook of Physical Constants*, 1995, p. 308.
- [22] G. Walter, U. Hoppe, J. Vogel, G. Cral, P. Hartmann, *J. Non-Cryst. Solids* 333 (2004) 252.
- [23] M. Colmont, L. Delevoye, E.M. Ketatni, L. Montagne, O. Mentré, *J. Solid State Chem.* 179 (2006) 2111.
- [24] I.V. Mardirosova, G.A. Bukhalova, *Russ. J. Inorg. Chem.* 11 (1966) 1275.
- [25] M. Tomozawa, *Phase Separation in Glass*, Academic Press, New York, 1979.
- [26] I. Elgayar, A.E. Aliev, A.R. Boccaccini, R.G. Hill, *J. Non-Cryst. Solids* 351 (2005) 173.
- [27] O.V. Mazurin (Ed.), *Phase Separation in Glasses*, 1984, p. 104.
- [28] H. Grussaute, L. Montagne, G. Palavit, J.L. Bernard, *J. Non-Cryst. Solids* 263/264 (2000) 312.
- [29] H. Grussaute, L. Montagne, G. Palavit, J. L. Bernard, *Glastech. Ber. Glass Sci. Technol.* 71C (1998) 204.
- [30] F.J. Ryerson, P.C. Hoss, *Geochim. Cosmochim. Acta* 44 (1979) 611.
- [31] P.W. McMillan, *Glass Ceramics*, second ed., Academic Press, New York, 1979, p. 151.